SUPPLEMENTARY INFORMATION

Seven supplementary figures with legends below.

SUPPLEMENTARY FIGURE LEGENDS

Figure S1 (related to Figure 1: Torin2 and omipalisib produce strong cytotoxic and anti-proliferative effects in TNBC cells). **A.** Quantitative western blotting of PTEN and INPP4B protein levels in 46 breast cancer and non-transformed mammary epithelial cell lines (see **Table S1**). The plot shows 48 data points because two independent protein lysates were prepared from SK-BR-3 cells and because MDA-MB-231 cells were cultured in two different types of media. Shown are mean values from at least 2 independent experiments. TNBC/basal-like cell lines are marked in red. Six TNBC/basal-like cell lines selected for more focused study are numbered. **B.** Cell counts at the beginning and end of the 72h treatment period were determined by co-staining with Hoechst (blue) and Live/Dead cell viability stain (red), followed by microscopy and image analysis (see STAR methods for details). Shown are representative images of HCC1806 cells following treatment with GR_{max} doses (3.2μM) of AZD8055 or Torin2 for 72h. Dead cells were identified based on pyknosis/karyorrhexis in the Hoechst channel and positive Live/Dead staining in the far red channel and excluded. Viable cell counts were then used to produce nine-point dose response curves, and GR metrics were computed to determine relative potency and efficacy. **C.** GR metrics quantify variation in drug potency and maximal efficacy. $GR_{max} > 0$ indicates partial growth inhibition, $GR_{max} = 0$ indicates complete growth inhibition, and $GR_{max} < 0$ indicates cytotoxicity. **D.** Clustergram heatmap of mean GR_{50} values for 24 drugs in six TNBC cell lines with PI3K pathway dysregulation; N=3 experiments, each performed in quadruplicate. The three drugs with the lowest GR_{max} values (**Figure 1B**) are highlighted in red. Trametinib (blue) is a MAPK pathway inhibitor included as a comparator. See **Table S3** for details on all drugs. **E.** GR_{max} values for a subset of PI3K pathway drugs including Torin2 in 7 luminal and 2 non-transformed mammary epithelial

cell lines. *P<0.05, **P<0.01, ***P<0.001, and n.s. (not significant) by Mann-Whitney U test. **F.** Growth curves for HCC1806 NLS-mCherry cells in the presence of GR_{max} concentrations of AZD8055, omipalisib and Torin2 (all 3.2μM) or 0.1xGR_{max} concentrations of Torin2 and omipalisib (0.32μM). Data points/shading indicate mean ± SD of 3 replicates in a single time-lapse experiment; N=3 experiments, representative data shown. "*" denotes start of treatment. **G.** Percentage of unlabeled nuclei after 48 or 75h of continuous labeling of HCC1806 cells with F-ara-EdU, starting after 24h of treatment. Drugs were used at GR_{max} concentrations (3.2μM) except for Torin2 and omipalisib, which were used at 0.3xGR_{max} (1μM) due to cell death at 3.2μM. Shown are the mean ± SEM; N=3 experiments (see **Figure 1E** for representative data from a single experiment). **H.** Representative images of Hs 578T cells in the presence or absence of a fluorescent reporter of caspase 3/7 activity. Cells were exposed to GR_{max} concentrations of AZD8055 (1μM) or Torin2 (3.2μM) for 24h, as indicated. Images are shown in greyscale for clarity. "BF" indicates brightfield image. Scale bar=400μm.

Figure S2 (related to Figure 2: PI3K/AKT/mTOR inhibitors impede progression of S phase.). A. p-AKT S473 levels in HCC1806 cells by immunofluorescence after 24h of drug exposure. Scale bar=50μm. **B.** Levels of p-AKT S473 in single cells. Boxplots show the median and 25th/75th percentiles. **C.** Mean ± SEM levels of six proteins/phosphoproteins whose values are expected to decrease with inhibition of PI3K pathway activity; N≥2 experiments, each performed in triplicate. Cell lines are as indicated. Protein/phosphoprotein levels were used to generate the clustergram heat maps shown in **Figure 2A** and calculate the signaling index values shown in **Figure S2D**. Measurements were performed by quantitative immunofluorescence microscopy after 24h of exposure to GR_{max} concentrations (1-3.2μM) of the indicated drugs. In HCC1806 cells only, Torin2 and omipalisib were used at 0.3xGR_{max} (1μM) due to cell death. Fluorescence intensity values were extracted from whole cells (p-AKT T308, p-AKT S473, p-GSK3β S9, p-4E-BP1 T37/46) or cytoplasmic (p-S6 S235/236) or

nuclear (cyclin D, FOXO3, p21 Cip1, p27 Kip1) compartments by image analysis. For each protein/phosphoprotein, background-subtracted fluorescence intensity measurements were normalized to values for DMSO. **D**. Mean ± SEM of signaling index values for the data shown in C. Index values range from 0 for complete inhibition to 9 for no difference from DMSO-only control (see STAR methods for details). **E.** Mean percent ± SEM of p-pRb-low HCC1806 cells t=T_d (28h); N=3 experiments. ***P<0.001 by one-way ANOVA and Tukey's test (only selected comparisons shown).

Figure S3 (related to Figure 2: PI3K/AKT/mTOR inhibitors impede progression of S phase.). A. Analysis of nuclear DNA content vs EdU content in BT-20 cells treated with 3.2μM alpelisib or DMSO. Colors indicate cell cycle stage: G1 (black), active S phase (red), S-phase non-replicating (S_{NR}; yellow), and G2/M (blue). Color scheme applies to data in panels B, E, F and H. **B.** Distribution of cells in different cell cycle stages in two additional TNBC/basal-like cell lines after exposure to the indicated treatments for t= T_d (32h for Hs 578T, 40h for BT-549). Drugs were used at GR_{max} doses (1-3.2μM) except for Torin2 and omipalisib, which were used at 0.3xGR_{max} concentrations (1μM) in Hs 578T cells due to cell death. Drugs are ordered by viable cell number at T_d, with the least effective on top and most effective on the bottom. **C.** DNA content vs mean nuclear EdU intensity after exposure of HCC1806 cells to Torin2 at 0.03-0.3xGR_{max} dose. DNA content distribution for gated EdU-negative cells (red box) is shown below. Black arrows denote S_{NR} cells. **D.** Mean ± SEM of active S vs. S_{NR} cells from data shown in C; N=3 experiments. **E**. DNA content vs. mean nuclear intensity values for p-pRb after exposure of HCC1806 cells to GR_{max} doses of AZD8055 or Torin2 for t=T_d. Colors indicate different cell cycle stages based on measurement of DNA content and EdU content in the same cells. **F.** Effects of submaximal concentrations (0.1-1xGR_{max}) of AZD8055 on the distribution of BT-549 cells in different cell cycle stages. Submaximal doses were used to analyze S-phase cells because few cells were in active S phase at GR_{max} doses (1μM). Cells were pulse-labeled with EdU for 60min. **G.** Bar graphs (left)

display the percentage of EdU-positive (active) S-phase cells in the entire cell population after treatment with DMSO or AZD8055 at the indicated doses. Boxplots overlaid onto single cell data (right) indicate the median and 25^{th}/75^{th} percentiles for nuclear EdU content in all S-phase cells (active S plus S_{NR}). **H.** Cell cycle analysis for BT-20 cells performed after 6h of exposure to the indicated drugs at GR_{max} concentrations (1-3.2μM). **I.** Quantification of nuclear EdU content in S-phase cells after 6h (0.125 x T_d) or 14h (0.3 x T_d) of drug exposure. ***P<0.001 vs DMSO control (Mann-Whitney U test).

Figure S4 (related to Figure 4: Torin2 causes replication catastrophe). A. Torin2 (but not omipalisib) increases the percentage of HCC70 cells with high levels of native BrdU, γH2A.X, and p-RPA at t= ~0.5xT_d (20-24h). Cells with increased nuclear levels appear in the red gate and are labeled red. Drugs were used at GR_{max} doses (1-3.2μM) except for Torin2, which was used at 0.3xGR_{max} (1μM). **B.** Bar graphs display the mean ± SEM; N=3 experiments. *P<0.05, **P<0.01, ***P<0.001 vs. DMSO by one-way ANOVA and Dunnett's test. **C.** DNA content vs. nuclear intensities of p-Chk1 S317 and p-Chk2 T68 after treating HCC1806 cells with the indicated drugs for ~0.2xT_d (5h). Cells with increased nuclear levels appear in the red gate and are labeled red. Quantification of independent experimental replicates appears in **Figure 4C**.

Figure S5 (related to Figure 5: The activity of Torin2 in TNBC results from combined antagonism of mTORC1/2 and PIKKs). A. Dose-response curves (72h) for AZD8055, Torin2, AZ20, and AZD8055/AZ20 mixed at equimolar concentrations in HCC1806 and HCC70 cells. **B.** Chemical structures of Torin1, Torin2 and nine Torin2 analogs. **C.** Levels of p-AKT S473, p-4E-BP1 T37/46 and γH2A.X at t=0.33xT_d (14h) vs. GR values computed after 72h of exposure of HCC70 cells to 0.032, 0.32, or 3.2μM of AZD8055, Torin1, Torin2 or Torin2 analogs. Drugs/doses whose GR values correlate with mTORC1/2 signaling activity fall on the black regression lines (*left, middle*). Drugs/doses whose

activities are discontinuous with the regression fall within the red boxes (*left, middle*) and cause increased levels of γH2A.X (*black box*, *right*). **D.** DNA content vs. nuclear γH2A.X or p-pRb levels at 14h for DMSO (#1) and drugs/doses whose activities correlate with mTORC1/2 signaling activity (#2-4) and those that do not (#5-8). Percentages of gated γH2A.X-high or p-pRb-low cells are relative to entire treated population. **E**. Mean percent ± SEM of γH2A.X-high cells or p-pRb-low cells at 14h post-treatment, based on data shown in D; N=3 experiments. *P<0.05, **P<0.01,***P<0.001 by one-way ANOVA and Dunnett's test.

Figure S6 (related to Figure 6: Combined inhibition of mTORC1/2 and PIKKs produces benefit by co-targeting pathways required in S phase). A. Results of analysis of interactions between PI3K pathway drugs and the Chk1 inhibitor rabusertib. "+" indicates additive or greater benefit by Loewe criteria, "N.I." indicates no interaction, and "ant." indicates antagonism. **B.** Dose ranges of drugs used for analysis of drug interactions. Ranges were selected based on the dose response curves for each single agent and reflect submaximal levels of drug effect (spanning the GR_{50} dose). **C.** Analysis of mTORC1/2 signaling after exposure of HCC70 or Hs 578T cells to 32-100nM of AZD8055, which is equivalent to 0.01-0.03xGR_{max} dose in HCC70 cells and 0.03-0.1xGR_{max} dose in Hs 578T cells. HCC70 and Hs 578T cells were exposed to drugs for t= ~0.5xT_d (24h) and for t=0.75xT_d (24h), respectively. The effects of 1μM Torin2 are shown for comparison.

Figure S7 (related to Figure 7. Low doses of mTORC1/2 and ATR/Chk1 inhibitors in combination cause increased ssDNA in mitotic prophase and death). A. Mitoses per high-powered field (h.p.f.) after exposure of HCC70 cells to the indicated drugs for t= ~0.5xT_d (24h). Mitoses were quantified by staining cells with Hoechst and anti-CREST, anti-β-tubulin, and anti-γ-tubulin antibodies. Bar graphs represent the mean ± SEM; N=3 experiments. Values were normalized to DMSO prior to averaging.

*P<0.05, **P<0.01, ***P<0.001 and n.s. (not significant) by ANOVA and Tukey's test (only selected comparisons shown). **B.** Mean percent ± SEM of cells in different stages of mitosis, as determined by immunofluorescence microscopy; N=3 experiments, 569 mitoses. *P<0.05, **P<0.01, ***P<0.001 and n.s. (not significant) by ANOVA and Tukey's test (only selected comparisons shown). **C.** Rate of mitotic entry (% of cells per hour) as determined by time-lapse imaging of asynchronous HCC70 H2B-GFP cells after 15 or 30h of exposure to the indicated treatments.

FIGURE S1

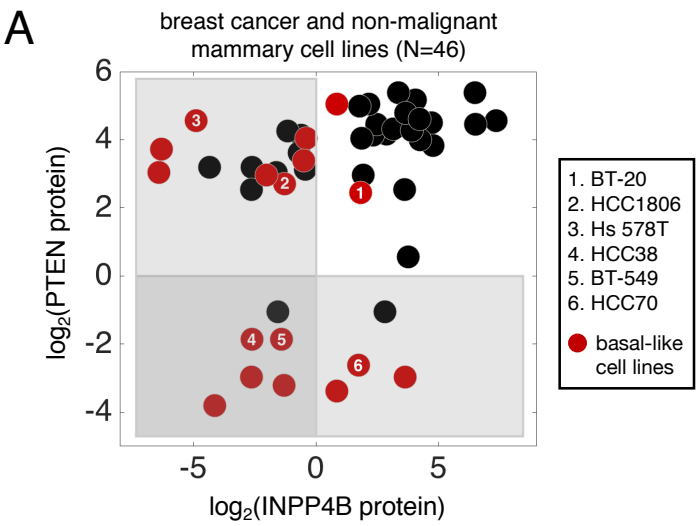
A
breast cancer and non-malignant mammary cell lines (N=46)
log2(PTEN protein)
log2(INPP4B protein)
1. BT-20
2. HCC1806
3. Hs 578T
4. HCC38
5. BT-549
6. HCC70
basal-like cell lines

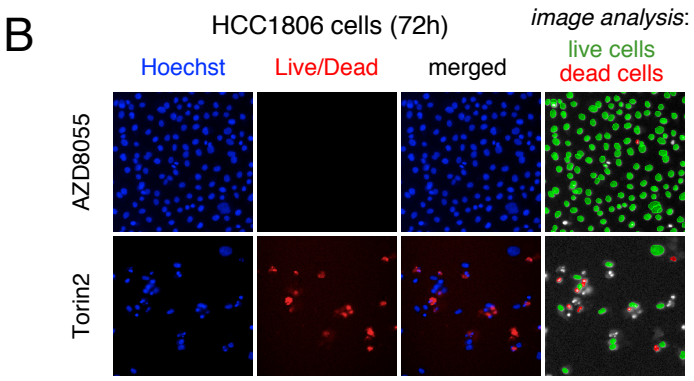
B
HCC1806 cells (72h)
image analysis:
live cells
dead cells
Hoechst
Live/Dead
merged
AZD8055
Torin2

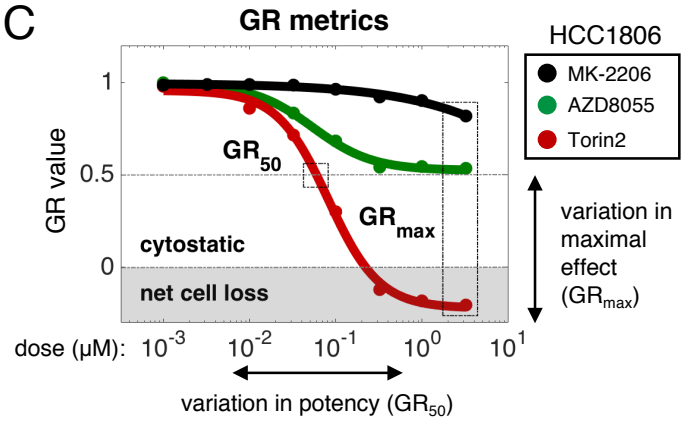
C
GR metrics
HCC1806
MK-2206
AZD8055
Torin2
GR value
GR50
GRmax
cytostatic
net cell loss
variation in maximal effect (GRmax)
dose (μM):
variation in potency (GR50)

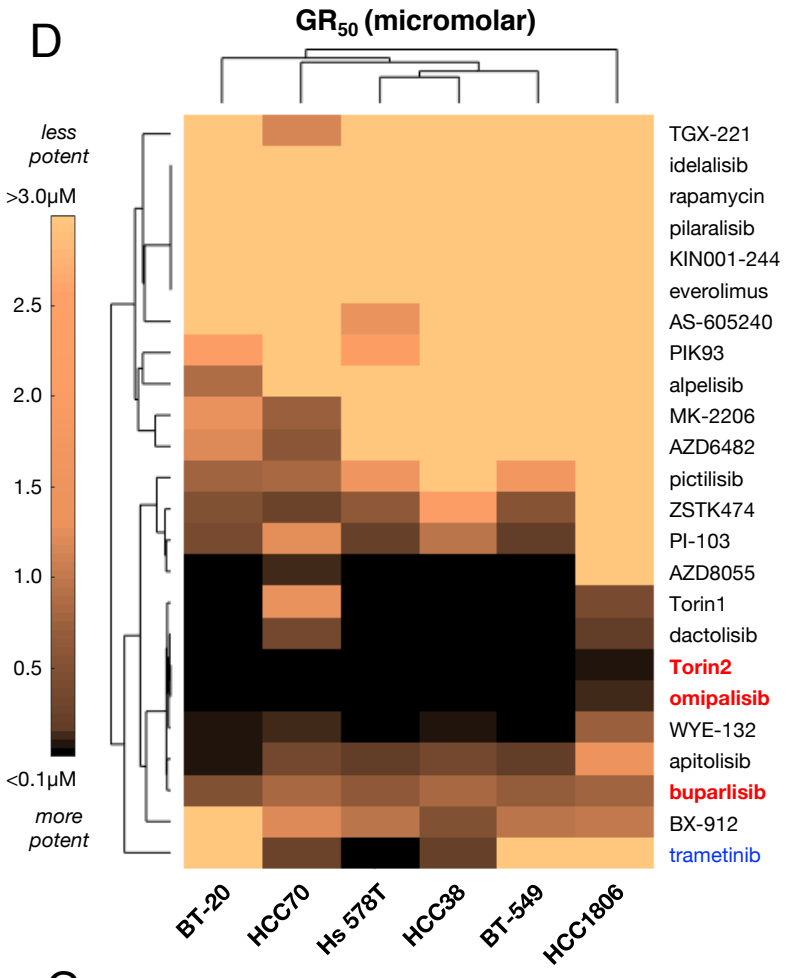
D
GR50 (micromolar)
less potent
>3.0μM
<0.1μM
more potent
TGX-221
idelalisib
rapamycin
pilaralisib
KIN001-244
everolimus
AS-605240
PIK93
alpelisib
MK-2206
AZD6482
pictilisib
ZSTK474
PI-103
AZD8055
Torin1
dactolisib
Torin2
omipalisib
WYE-132
apitolisib
buparlisib
BX-912
trametinib
BT-20
HCC70
Hs 578T
HCC38
BT-549
HCC1806

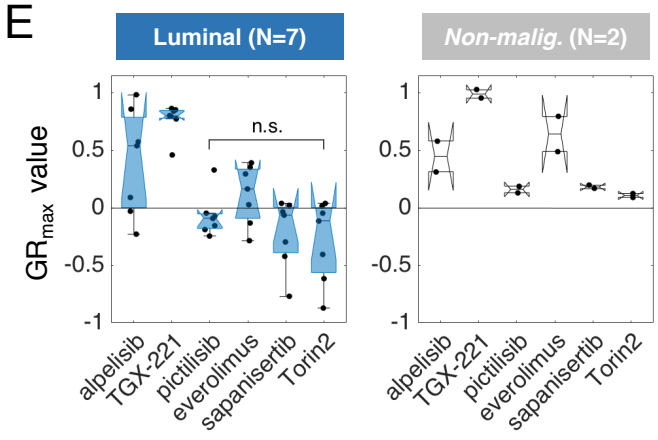
E
Luminal (N=7)
Non-malig. (N=2)
GRmax value
n.s.
alpelisib
TGX-221
pictilisib
everolimus
sapanisertib
Torin2

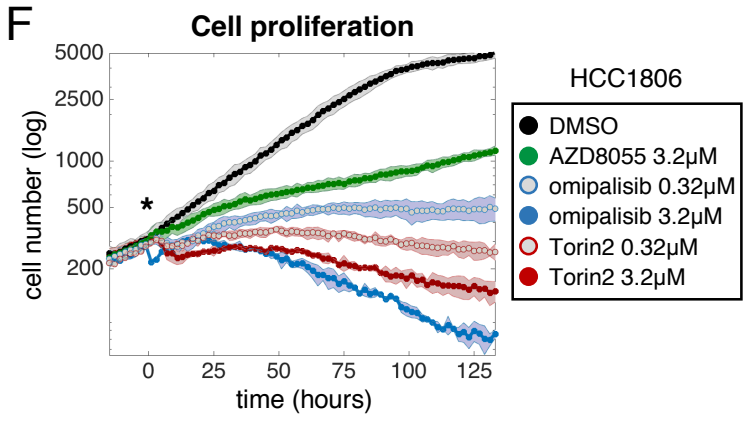
F
Cell proliferation
HCC1806
DMSO
AZD8055 3.2μM
omipalisib 0.32μM
omipalisib 3.2μM
Torin2 0.32μM
Torin2 3.2μM
cell number (log)
time (hours)

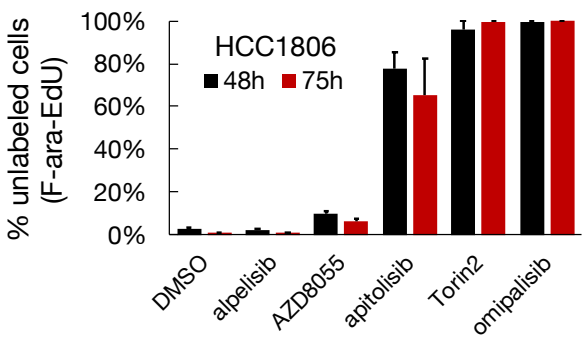
G
% unlabeled cells (F-ara-EdU)
HCC1806
48h
75h
DMSO
alpelisib
AZD8055
apitolisib
Torin2
omipalisib

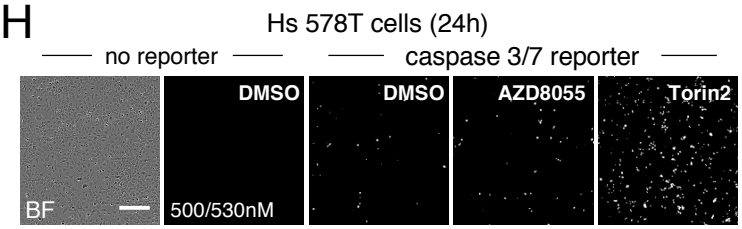
H
Hs 578T cells (24h)
no reporter
caspase 3/7 reporter
DMSO
DMSO
AZD8055
Torin2
BF
500/530nM

FIGURE S2

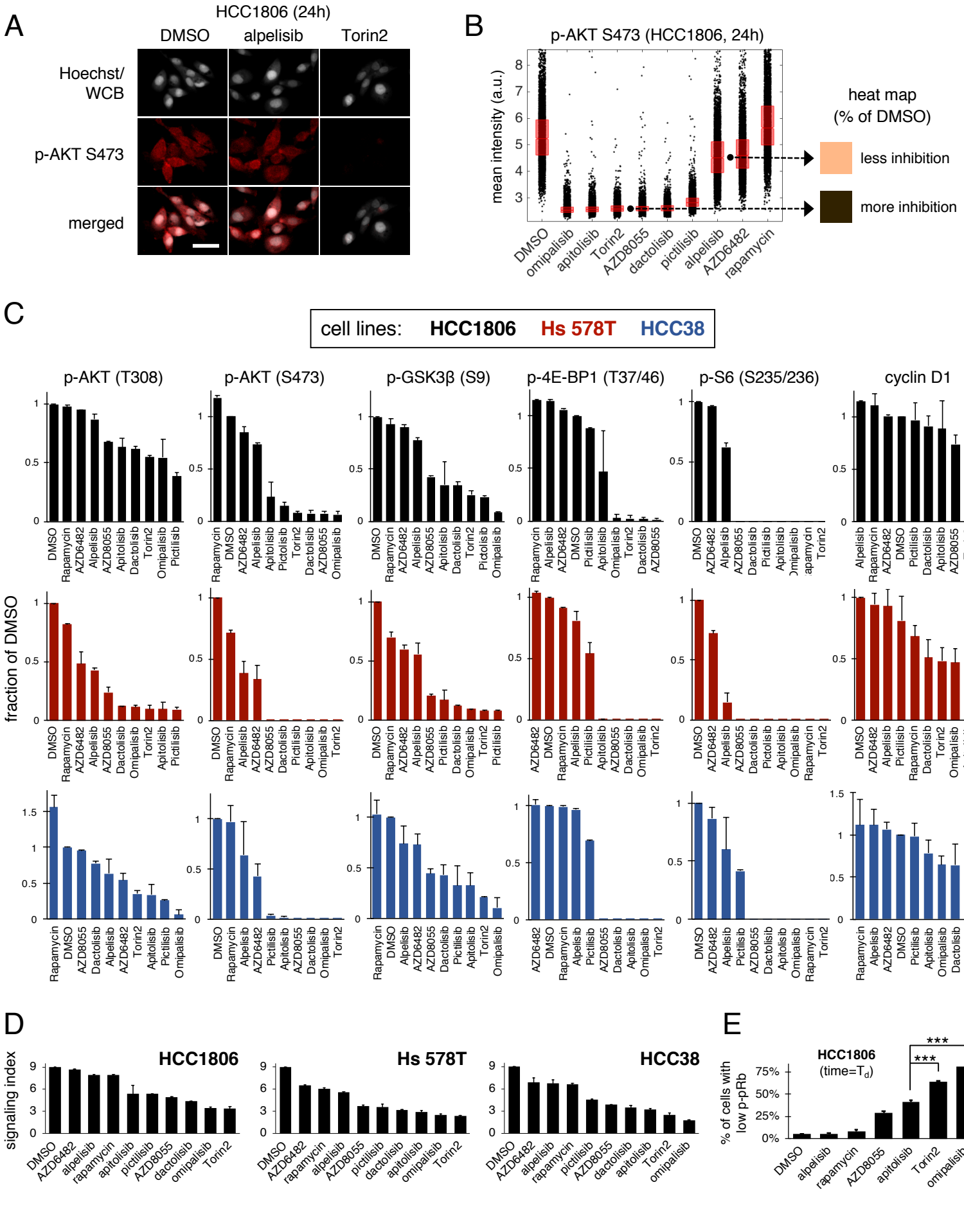
A
HCC1806 (24h)
DMSO
alpelisib
Torin2
Hoechst/ WCB
p-AKT S473
merged
B
p-AKT S473 (HCC1806, 24h)
mean intensity (a.u.)
heat map (% of DMSO)
less inhibition
more inhibition
DMSO
omipalisib
apitolisib
Torin2
AZD8055
dactolisib
pictilisib
alpelisib
AZD6482
rapamycin
C
cell lines: HCC1806 Hs 578T HCC38
p-AKT (T308)
p-AKT (S473)
p-GSK3β (S9)
p-4E-BP1 (T37/46)
p-S6 (S235/236)
cyclin D1
fraction of DMSO
D
signaling index
HCC1806
Hs 578T
HCC38
E
% of cells with low p-pRb
HCC1806 (time=Td)
***
***

FIGURE S3

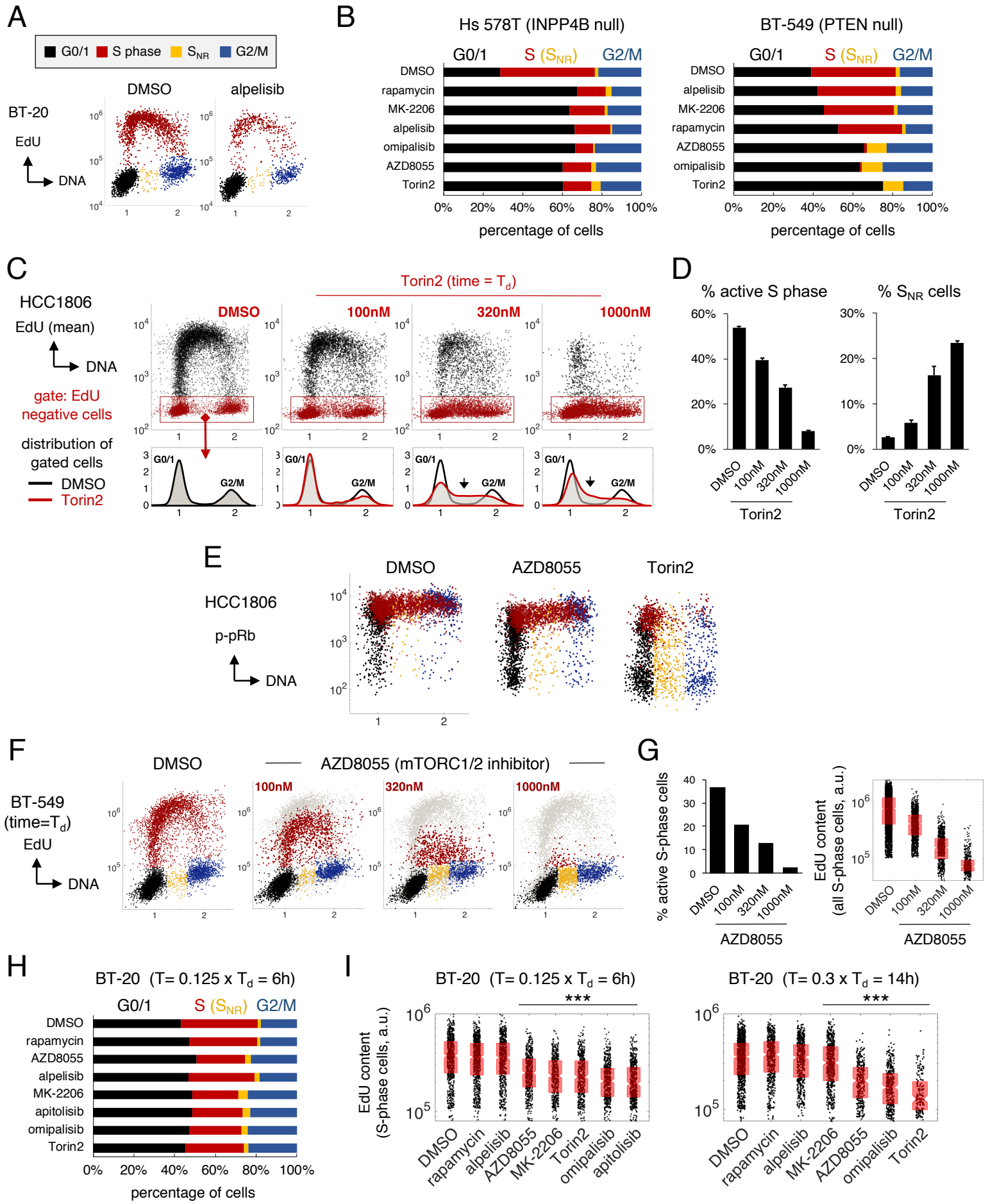
A
G0/1
S phase
S_NR
G2/M
DMSO
alpelisib
BT-20
EdU
DNA
B
Hs 578T (INPP4B null)
BT-549 (PTEN null)
G0/1
S (S_NR)
G2/M
DMSO
rapamycin
MK-2206
alpelisib
omipalisib
AZD8055
Torin2
0%
20%
40%
60%
80%
100%
percentage of cells
C
HCC1806
EdU (mean)
DNA
gate: EdU negative cells
distribution of gated cells
DMSO
Torin2
Torin2 (time = T_d)
DMSO
100nM
320nM
1000nM
G0/1
G2/M
D
% active S phase
% S_NR cells
60%
40%
20%
0%
30%
20%
10%
0%
DMSO
100nM
320nM
1000nM
Torin2
E
HCC1806
p-pRb
DNA
DMSO
AZD8055
Torin2
F
DMSO
AZD8055 (mTORC1/2 inhibitor)
BT-549
(time=T_d)
EdU
DNA
100nM
320nM
1000nM
G
% active S-phase cells
EdU content
(all S-phase cells, a.u.)
DMSO
100nM
320nM
1000nM
AZD8055
H
BT-20 (T= 0.125 x T_d = 6h)
G0/1
S (S_NR)
G2/M
DMSO
rapamycin
AZD8055
alpelisib
MK-2206
apitolisib
omipalisib
Torin2
0%
20%
40%
60%
80%
100%
percentage of cells
I
BT-20 (T= 0.125 x T_d = 6h)
BT-20 (T= 0.3 x T_d = 14h)
***
EdU content
(S-phase cells, a.u.)
DMSO
rapamycin
alpelisib
AZD8055
MK-2206
Torin2
omipalisib
apitolisib

FIGURE S4

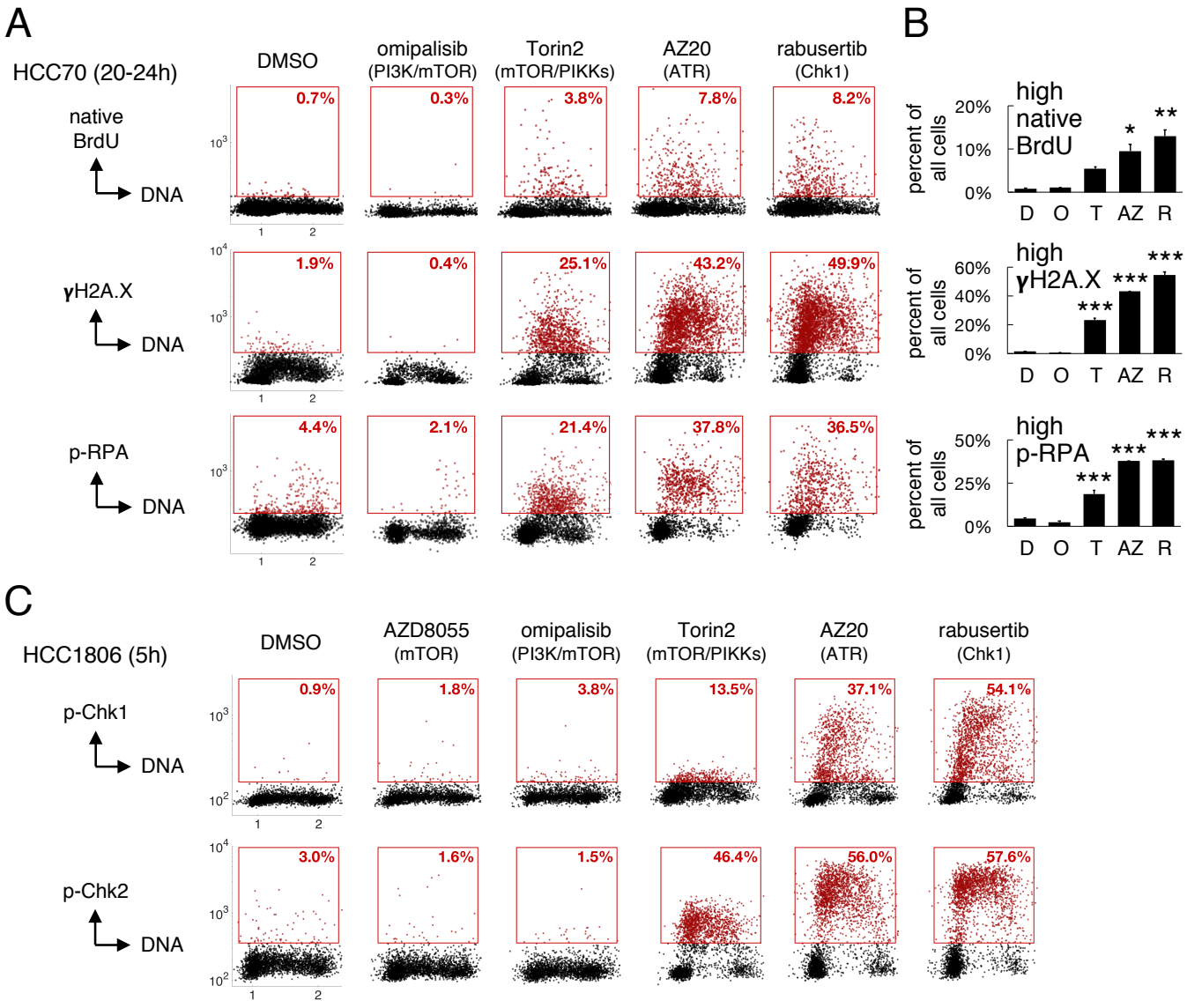
A
HCC70 (20-24h)
DMSO
omipalisib (PI3K/mTOR)
Torin2 (mTOR/PIKKs)
AZ20 (ATR)
rabusertib (Chk1)
native BrdU
γH2A.X
p-RPA
DNA
0.7%
0.3%
3.8%
7.8%
8.2%
1.9%
0.4%
25.1%
43.2%
49.9%
4.4%
2.1%
21.4%
37.8%
36.5%
B
high native BrdU
high γH2A.X
high p-RPA
percent of all cells
D O T AZ R
C
HCC1806 (5h)
DMSO
AZD8055 (mTOR)
omipalisib (PI3K/mTOR)
Torin2 (mTOR/PIKKs)
AZ20 (ATR)
rabusertib (Chk1)
p-Chk1
p-Chk2
0.9%
1.8%
3.8%
13.5%
37.1%
54.1%
3.0%
1.6%
1.5%
46.4%
56.0%
57.6%

FIGURE S5

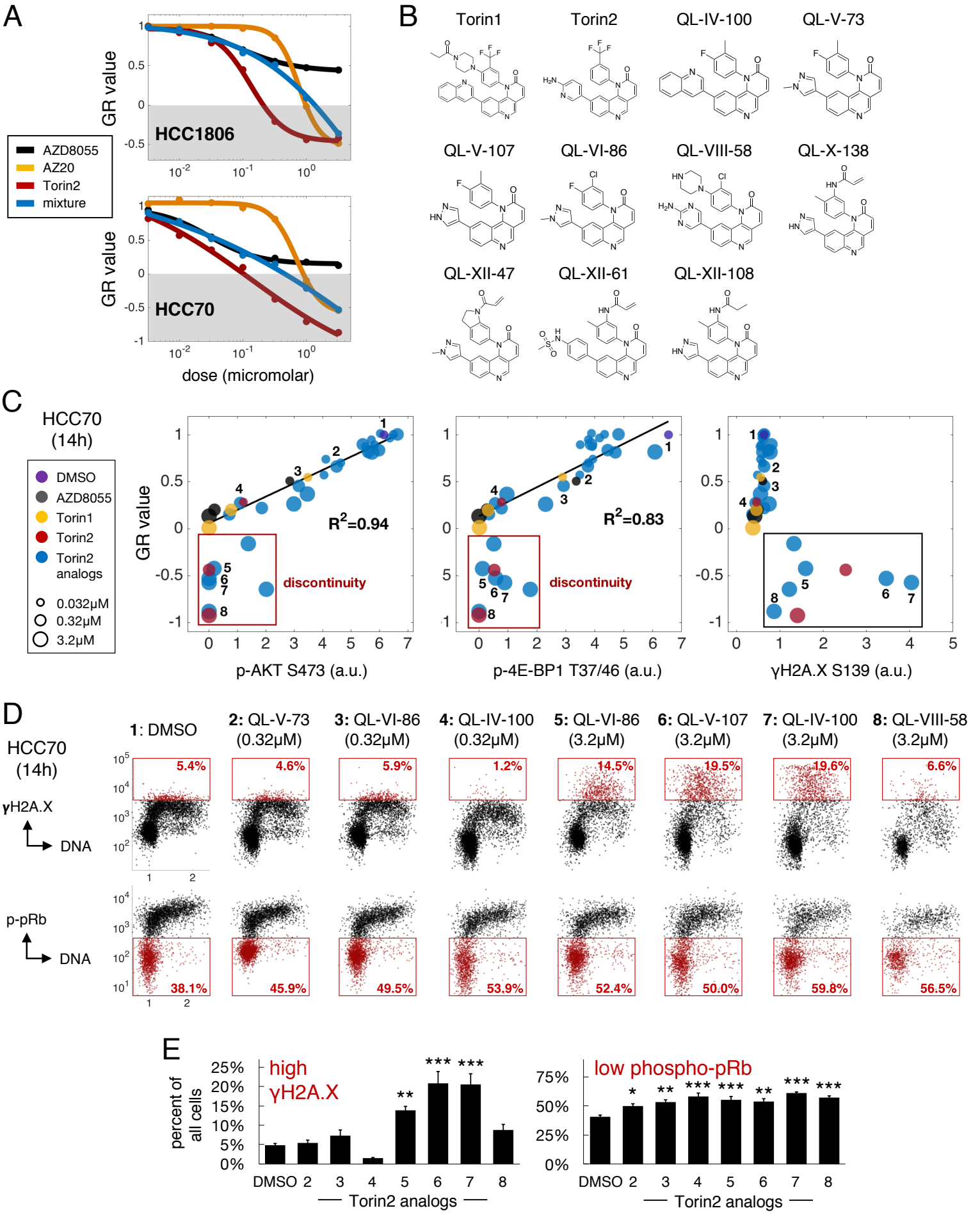
A
GR value
HCC1806
HCC70
AZD8055
AZ20
Torin2
mixture
dose (micromolar)
B
Torin1
Torin2
QL-IV-100
QL-V-73
QL-V-107
QL-VI-86
QL-VIII-58
QL-X-138
QL-XII-47
QL-XII-61
QL-XII-108
C
HCC70
(14h)
DMSO
AZD8055
Torin1
Torin2
Torin2
analogs
0.032μM
0.32μM
3.2μM
GR value
R2=0.94
R2=0.83
discontinuity
p-AKT S473 (a.u.)
p-4E-BP1 T37/46 (a.u.)
γH2A.X S139 (a.u.)
D
HCC70
(14h)
1: DMSO
2: QL-V-73
(0.32μM)
3: QL-VI-86
(0.32μM)
4: QL-IV-100
(0.32μM)
5: QL-VI-86
(3.2μM)
6: QL-V-107
(3.2μM)
7: QL-IV-100
(3.2μM)
8: QL-VIII-58
(3.2μM)
γH2A.X
DNA
p-pRb
DNA
5.4%
4.6%
5.9%
1.2%
14.5%
19.5%
19.6%
6.6%
38.1%
45.9%
49.5%
53.9%
52.4%
50.0%
59.8%
56.5%
E
high
γH2A.X
low phospho-pRb
percent of
all cells
DMSO 2 3 4 5 6 7 8
Torin2 analogs

FIGURE S6

A

rabusertib (Chk1i)

	HCC70	Hs 578T	BT-549	HCC1806	BT-20
AZD6482	NI	NI	NI	NI	+
AZD8055	+	+	+	+	+
buparlisib	NI	NI	NI	NI	+
alpelisib	NI	NI	NI	NI	+
apitolisib	+	+	+	+	+
MK-2206	+	NI	NI	NI	+
rapamycin	NI	NI	+	NI	+
WYE-132	+	+	+	+	+

B

dose ranges evaluated

	HCC70	**Hs 578T**	**BT-549**	**HCC1806**	**BT-20**
AZ20	100-1000	320-3200	320-3200	100-1000	320-3200
rabusertib	100-1000	100-1000	320-3200	60-600	1000-5600
AZD6482	3.2-100	320-3200	320-3200	100-1000	320-3200
AZD8055	10-200	10-200	10-200	10-1000	10-320
buparlisib	100-1000	100-1000	100-1000	100-1000	100-1000
alpelisib	320-3200	320-3200	320-3200	320-3200	320-3200
apitolisib	3.2-320	32-320	32-2000	100-3200	32-320
MK-2206	100-1000	320-3200	100-3200	320-3200	320-3200
rapamycin	100-1000	100-1000	100-1000	100-1000	100-1000
WYE-125	10-200	10-200	10-400	10-1000	10-320

C

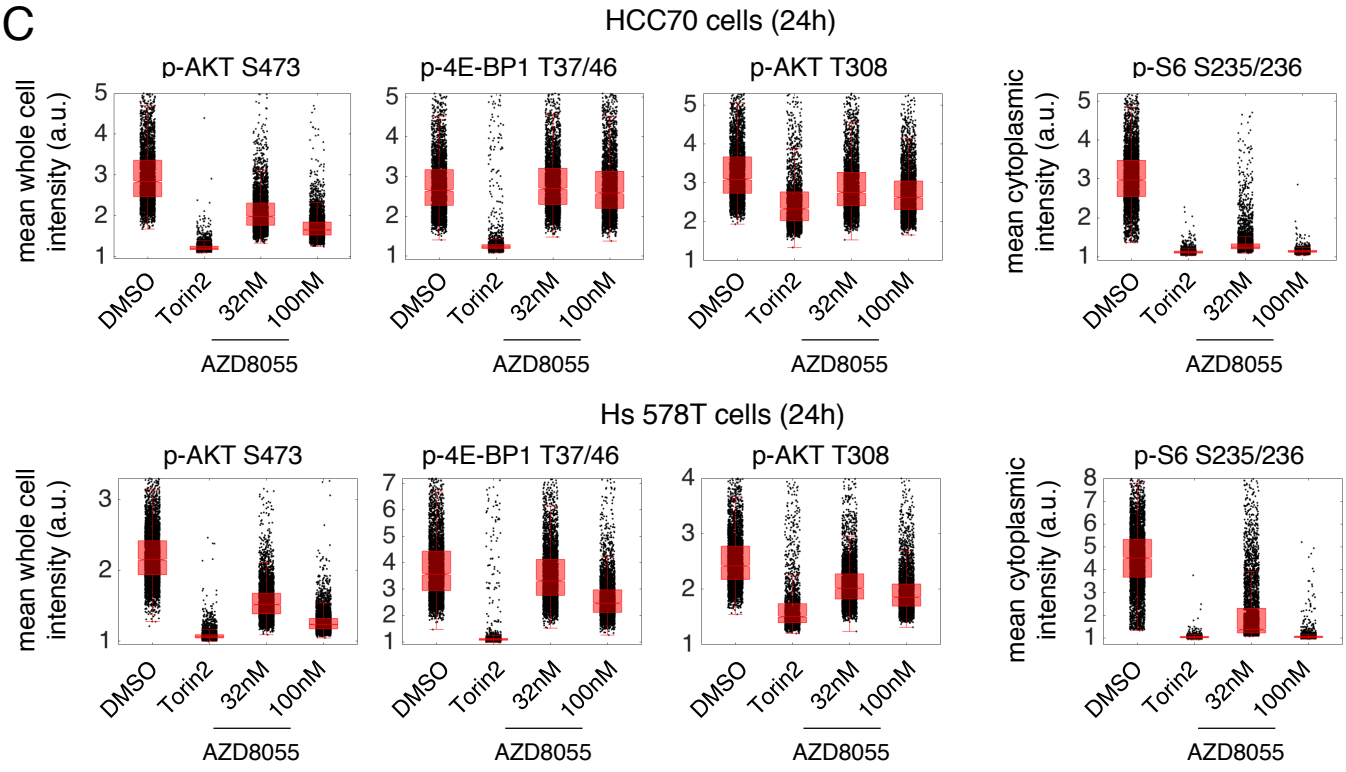

FIGURE S7

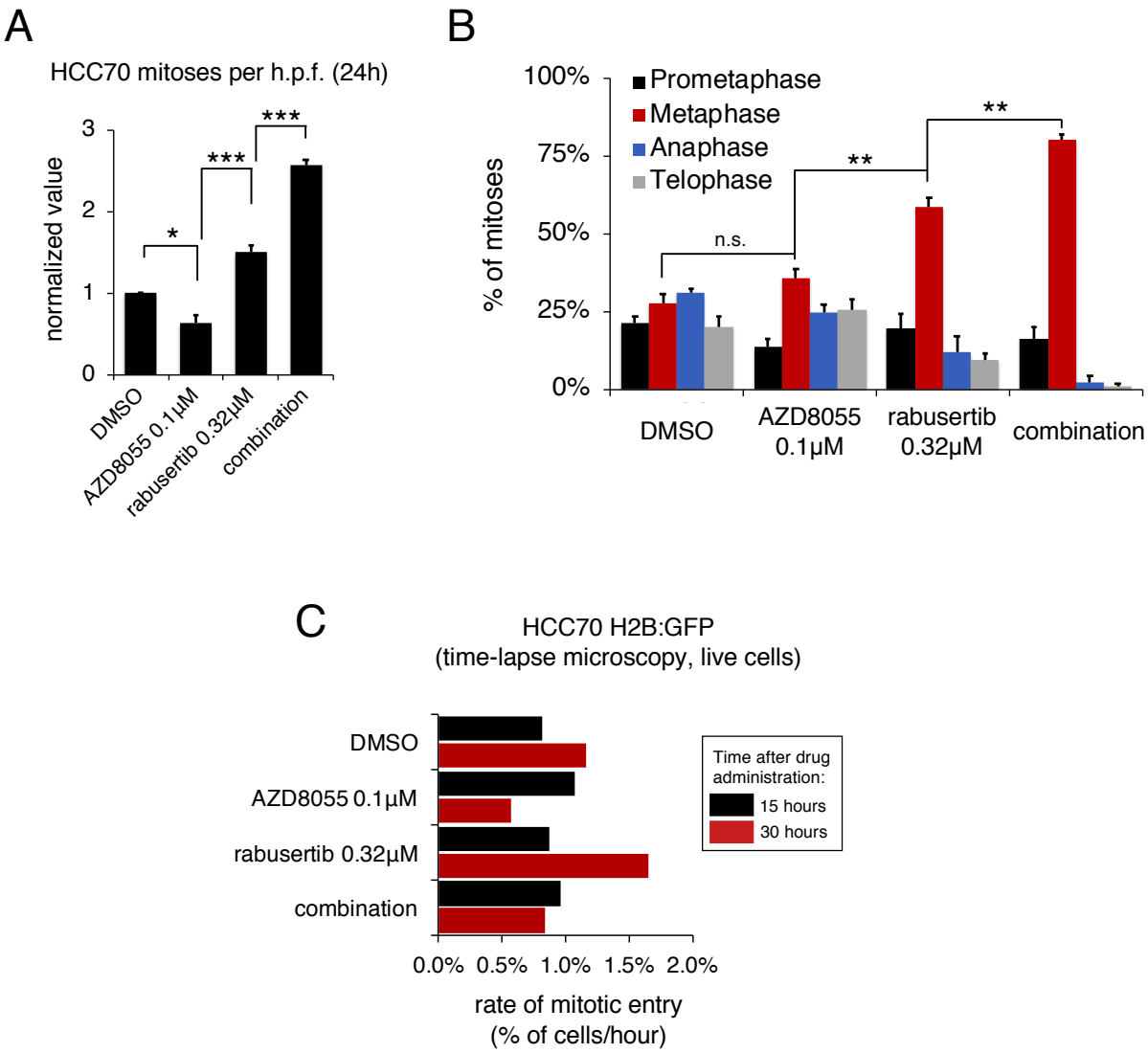
A
HCC70 mitoses per h.p.f. (24h)
normalized value
0
1
2
3
*
***
***
DMSO
AZD8055 0.1μM
rabusertib 0.32μM
combination
B
% of mitoses
100%
75%
50%
25%
0%
Prometaphase
Metaphase
Anaphase
Telophase
n.s.
**
**
DMSO
AZD8055 0.1μM
rabusertib 0.32μM
combination
C
HCC70 H2B:GFP
(time-lapse microscopy, live cells)
DMSO
AZD8055 0.1μM
rabusertib 0.32μM
combination
Time after drug administration:
15 hours
30 hours
0.0% 0.5% 1.0% 1.5% 2.0%
rate of mitotic entry
(% of cells/hour)

Table S1 (related to Figure 1): Classification of breast cancer and non-transformed mammary epithelial cell lines used in this study. 46 cell lines used to assess PTEN and INPP4B protein levels by quantitative western blotting are marked with #. Six TNBC/basal-like cell lines with PI3K pathway activation used for quantitative analysis of responses to PI3K pathway inhibitors appear in **BOLD.** 28 cell lines (*i.e.*, 19 basal-like, 7 luminal and 2 non-transformed mammary epithelial cell lines) used for follow-up studies of drug sensitivity are marked with &.

Cell lines	Gene expression	*HER2* amplified
184-B5#	Basal[4]	n/a
AU-565#	Luminal[1]	Y[1]
BT-20#,&	Basal A[1]	N[1]
BT-474#	Luminal[1]	Y[1]
BT-483#	Luminal[1]	N[1]
BT-549#,&	Basal B[1]	N[1]
CAL-120&	Basal B[5]	n/a
CAL-51&	Basal B[2]	N[2]
CAL-85-1&	Basal-like 2[3]	n/a
CAMA-1#,&	Luminal[1]	N[1]
HCC1143&	Basal A[1]	N[1]
HCC1395#,&	Basal B[2]	N[2]
HCC1419#	Luminal[2]	Y[2]
HCC1428#,&	Luminal[1]	N[1]
HCC1500#,&	Luminal[2]	N[1]
HCC1569#	Basal A[1]	Y[1]
HCC1806#,&	Basal-like 2[3]	N[2]
HCC1937#,&	Basal A[1]	N[1]
HCC1954#	Basal A[1]	Y[1]
HCC202#	Luminal[2]	Y[1]
HCC38#,&	Basal B[1]	N[1]
HCC70#,&	Basal A[1]	N[1]
hTERT-HME1&	Basal B[2]	N[2]
Hs 578T#,&	Basal B[1]	N[1]
MCF-10A#,&	Basal B[1]	N[1]
MCF10DCIS#	n/a	n/a
MCF-10F#	n/a	n/a
MCF-12A#	Basal B[1]	N[1]
MCF-7#,&	Luminal[1]	N[1]
MDA-MB-134#,&	Luminal[1]	N[1]
MDA-MB-157#,&	Basal B[1]	N[1]
MDA-MB-175#	Luminal[1]	N[1]
MDA-MB-231#,&	Basal B[1]	N[1]
MDA-MB-361#	Luminal[1]	Y[1]
MDA-MB-415#	Luminal[1]	N[1]
MDA-MB-436#,&	Basal B[1]	N[1]
MDA-MB-453#,&	Luminal[1]	N[1]
MDA-MB-468#,&	Basal A[1]	N[1]
SK-BR-3#	Luminal[1]	Y[1]
SUM102PT#	Basal B[2]	N[2]
SUM1315#,&	Basal B[1]	N[1]
SUM149PT#,&	Basal B[1]	N[1]
SUM159PT#,&	Basal B[1]	N[1]
SUM225CWN#	Basal A[1]	Y[1]
SUM44PE#	Luminal[1]	Y[2]
SUM52PE#	Luminal[1]	Y[1]
T-47D#,&	Luminal[1]	N[1]
UACC-812#	Luminal[1]	Y[1]
UACC-893#	Luminal[2]	Y[1]
ZR-75-1#	Luminal[1]	N[1]
ZR-75-30#	Luminal[1]	Y[1]

REFERENCES

[1]Neve RM, et al. (2006) *Cancer Cell* 10:515-527.
[2]Kao J, et al. (2009) *PLoS ONE* 4:e6146.
[3]Lehmann BD, et al. (2011) *J Clin Invest* 121:2750-67.
[4]Charafe-Jauffret, et al. (2006) *Oncogene* 25:2273-2284.
[5]Dai X, et al. (2017) *J Cancer* 8:3131-3141.

Table S2 (related to Figure 1): Molecular characteristics of the six TNBC/basal-like cell lines selected for quantitative analysis of responses to PI3K pathway inhibitors.

TNBC cell lines	PI3K pathway (mutated gene)	Nucleotide variant	Amino acid substitution	PTEN, INPP4B protein level (rank)[4]	*TP53* mutation[5] (cDNA, protein)
BT-20	*PIK3CA*	c.3140A>G[1] c.1616C>G[1]	p.H1047R p.P539R	2.44 (37) 1.83 (23)	c.394A>C[1] p.K132Q
BT-549	*PTEN*	c.823delG[1]	p.V275fs*1	-1.85 (42) -1.41 (36)	c.747G>C[1] p.R249S
HCC1806	*INPP4B*	c.2541C>G[2]	p.D847E[3]	2.70 (34) -1.29 (34)	c.766_767insAA[1] p.T256fs*90
HCC38	*PIK3CA*	c.1157G>T[2]	p.W386L	-1.85 (41) -2.62 (40)	c.818G>T[1] p.R273L
HCC70	*PTEN*	c.270delT[1]	p.F90fs*9	-2.62 (43) 1.74 (25)	c.743G>A[1] p.R248Q
Hs 578T	*PIK3R1*	c.1358_1359 insTAA[1]	p.N453_T454 insN	4.57 (10) -4.89 (46)	c.469G>T[1] p.V157F

[1]Reported by ATCC.
[2]Reported in COSMIC (searched through canSAR 4.0)
[3]Loss of function substitution according to Lopez SM, et al. *Biochem Biophys Res Commun*, 2013.
[4]Log base 2 of the mean protein level assessed by quantitative western blotting. ( ) = rank in a panel of 48 lysates from 46 breast cancer and non-transformed mammary epithelial cell lines (see **Table S1**), with 1 and 48 assigned to the highest and lowest values, respectively.
[5]All cell lines are homozygous for *TP53* mutations.

Table S3 (related to Figure 1): Drug compounds used in this study (N=31). The initial analysis of drug responses used 23 PI3K pathway inhibitors and the MEK inhibitor trametinib (see **BOLD**). Sapanisertib was added during follow-up studies. Six inhibitors of DNA damage response pathways were also used in follow-up studies.

Compound	Generic name	Clinical development	Phase[#]	Nominal targets
AS-605240	n/a	N	n/a	PI3K p110γ
AZD2281	olaparib	Y	1-3; FDA-approved	PARP1/2
AZD6482	n/a	Y[1]	1	PI3K p110β
AZD8055	n/a	Y	1[#]	mTORC1/2
AZ20	n/a	N	n/a	ATR
BEZ235	dactolisib	Y	1-2	PI3K p110(α,β,δ,γ), mTORC1/2, ATR
BKM120	buparlisib	Y	1-3	PI3K p110(α,β,δ,γ)
BYL719	alpelisib	Y	1-3	PI3K p110α
BX-912	n/a	N	n/a	PDK1
CAL-101 (GS-1101)	idelalisib	Y	1-3; FDA-approved	PI3K p110δ
GDC-0941	pictilisib	Y	1-2[#]	PI3K p110(α,β,δ,γ)
GDC-0980	apitolisib	Y	1-2	PI3K p110(α,β,δ,γ), mTORC1/2
GSK1120212	trametinib	Y	1-3; FDA-approved	MEK1/2
GSK2126458	omipalisib	Y	1[#]	PI3K p110(α,β,δ,γ), mTORC1/2
KIN001-244	n/a	N	n/a	PDK1
KU-60019	n/a	N	n/a	ATM
LY2603618	rabusertib	Y	1-2[#]	Chk1
MK-2206	n/a	Y	1-2	Akt1/2/3
MLN0128 (INK-128)	sapanisertib	Y	1-2	mTORC1/2
NU7026	n/a	N	n/a	DNA-PK
PI-103	n/a	N	n/a	PI3K p110(α,β,δ,γ), mTORC1/2, DNA-PK
PIK-93	n/a	N	n/a	PI3K p110α, p110γ; PI4KIIIβ
RAD001	everolimus	Y	1-3; FDA-approved	mTORC1
rapamycin	sirolimus	Y	1-3	mTORC1
TGX-221	n/a	N	n/a	PI3K p110β
Torin1	n/a	N	n/a	mTORC1/2, DNA-PK
Torin2	n/a	N	n/a	mTORC1/2, ATR, ATM, DNA-PK
VE-821	n/a	N	n/a	ATR
WYE-132	n/a	N	n/a	mTORC1/2
XL147 (SAR245408)	pilaralisib	Y	1-2	PI3K p110(α,β,δ,γ)
ZSTK474	n/a	Y	1[#]	PI3K p110(α,β,δ,γ)

[#]Indicates no active clinical trials (clinicaltrials.gov).
[1]Studied in patients for anti-platelet effects.

Table S4 (related to Figure 2): Downregulated (blue) and upregulated (red) metabolites in BT-549 cells following 6 hours of exposure to 1μM rapamycin, AZD8055, or Torin2, as identified by targeted metabolomics profiling. Analysis was performed using MetaboAnalyst 4.0 (see STAR methods for details).

Rapamycin (volcano plot cut-offs: fold change 1.5 and p-value 0.12):

metabolite	KEGG/HMDB ID	metabolic pathway	fold change	$\log_2$ (fold change)	raw p value	$-\log_{10}$ (p value)
1,3-diphosphateglycerate	C00236	glycolysis	0.17506	-2.5141	0.005024	2.2989
glycerophosphocholine	C00670	glycerophospholipid metabolism	0.30941	-1.6924	0.006531	2.185
2,3-diphosphoglyceric acid	C01159	glycolysis	0.42366	-1.239	0.088396	1.0536
UTP-nega	C00075	pyrimidine metabolism	0.47819	-1.0644	0.079647	1.0988
dTDP-nega	C00363	pyrimidine metabolism	0.49717	-1.0082	0.1124	0.94924
dGTP	C00286	purine metabolism	0.51058	-0.96978	0.096791	1.0142
NADPH-nega	C00005	glutathione metabolism	0.5184	-0.94785	0.057813	1.238
CDP-choline	C00307	glycerophospholipid metabolism	0.56569	-0.82192	0.057738	1.2385
CMP	C00055	pyrimidine metabolism	0.57775	-0.79148	0.10558	0.97642
carbamoyl phosphate	C00169	pyrimidine metabolism	0.59182	-0.75676	0.10358	0.98473
5-methoxytryptophan	HMDB02339	tryptophan metabolism	0.60642	-0.72162	0.034779	1.4587
glutamine	C00064	purine/pyrimdine metabolism, others	1.5486	0.63099	0.037744	1.4232
p-hydroxybenzoate	C00156	benzoate degradation	1.6104	0.68743	0.078678	1.1041
kynurenine	C00328	tryptophan metabolism	1.7086	0.77283	0.081955	1.0864
cytosine	C00380	pyrimidine metabolism	1.8465	0.8848	0.012569	1.9007
N-acetylputrescine	C02714	arginine and proline metabolism	2.004	1.0029	0.028281	1.5485
cytidine	C00475	pyrimidine metabolism	2.0479	1.0341	0.013472	1.8706
dTMP	C00364	pyrimidine metabolism	2.5661	1.3596	0.031743	1.4983

Metabolites detectable in all DMSO control samples but not in all treated samples (shown are peak intensity values):

metabolites	DMSO_1	DMSO_2	DMSO_3	Rapamycin_1	Rapamycin_2	Rapamycin_3
FMN	13817.8342	9204.51331	13128.728	6150.84896	NA	NA
cyclic bis(3->5) dimeric GMP	7676.66828	3390.80843	14429.9837	NA	NA	NA
succinyl-CoA-methylmalonyl-CoA-nega	5090.87455	5085.01944	8670.18606	NA	NA	NA
diiodothyronine	8350.47985	6784.31051	4675.54214	NA	NA	NA

AZD8055 (volcano plot cut-offs: fold change 1.5 and p-value 0.12):

metabolite	KEGG/HMDB ID	metabolic pathway	fold change	$\log_2$ (fold change)	raw p value	$-\log_{10}$ (p value)
2,3-diphosphoglyceric acid	C01159	glycolysis	0.33203	-1.5906	0.052983	1.2759
N-carbamoyl-L-aspartate-nega	C00438	pyrimidine metabolism	0.57796	-0.79095	0.11241	0.94921
dGDP-nega	C00361	purine metabolism	0.6014	-0.73361	0.11961	0.92221
dTDP-nega	C00363	pyrimidine metabolism	0.61724	-0.6961	0.083038	1.0807
N-acetyl-L-alanine	C01073	beta-alanine metabolism	0.65304	-0.61475	0.11847	0.92639
4-aminobutyrate	C00334	alanine, aspartate & glutamate metabolism	0.65956	-0.60043	0.054075	1.267
IDP-nega	C00104	purine metabolism	0.66408	-0.59057	0.11967	0.92201
phenylpropiolic acid	HMDB00563	phenylalanine metabolism	1.6197	0.69575	0.10052	0.99776
3-S-methylthiopropionate	C08276	cysteine & methionine metabolism	1.6749	0.74411	0.0093521	2.0291
5-methyl-THF	C00440	one carbon pool by folate	1.7904	0.8403	0.11602	0.93546
malonyl-CoA-posi	C00083	fatty acid biosynthesis	1.8578	0.89362	0.017418	1.759
N-acetylputrescine	C02714	arginine & proline metabolism	2.0599	1.0426	0.071022	1.1486
dTMP	C00364	pyrimidine metabolism	2.0744	1.0527	0.044968	1.3471
cytosine	C00380	pyrimidine metabolism	2.1107	1.0778	0.0002731	3.5638
deoxyinosine	C05512	purine metabolism	2.133	1.0929	0.020202	1.6946
D-sedoheptulose-1-7-phosphate	C05382	pentose phosphate pathway	2.7239	1.4457	0.022382	1.6501
cytidine	C00475	pyrimidine metabolism	3.0225	1.5958	0.0001058	3.9754
S-methyl-5-thioadenosine	C00170	cysteine & methionine metabolism	3.2664	1.7077	0.001777	2.7503
hypoxanthine	C00262	purine metabolism	4.9622	2.311	0.05315	1.2745

Metabolites detectable in all DMSO control samples but not in all treated samples (shown are peak intensity values):

metabolites	DMSO_1	DMSO_2	DMSO_3	AZD8055_1	AZD8055_2	AZD8055_3
FMN	13817.834	9204.5133	13128.728	12843.701	NA	NA
cyclic bis(3->5) dimeric GMP	7676.6683	3390.8084	14429.984	NA	NA	NA
succinyl-CoA-methylmalonyl-CoA-nega	5090.8746	5085.0194	8670.1861	NA	NA	NA
glycine	26286.235	7645.5868	19907.092	NA	NA	16124.418
choline	2871318.1	804003.85	2266906.1	4928666.6	NA	NA
5-methoxytryptophan	11870.832	7628.6091	13568.743	5948.8763	NA	NA
diiodothyronine	8350.4798	6784.3105	4675.5421	NA	NA	NA
retinoic acid	14769.437	6658.804	3700.0403	NA	NA	3813.5295

Table S4 (related to Figure 2), *continued*

Torin2 (volcano plot cut-offs: fold change 1.5 and p-value 0.12):

metabolite	KEGG/HMDB ID	metabolic pathway	fold change	$\log_2$ (fold change)	raw p value	$-\log_{10}$ (p value)
NADH	C00004	oxidative phosphorylation	0.30588	-1.709	0.094691	1.0237
dTDP-nega	C00363	pyrimidine metabolism	0.31052	-1.6873	0.0073083	2.1362
glyoxylate	C00048	glyoxylate & dicarboxylate metabolism	0.31628	-1.6607	0.066986	1.174
nicotinamide ribotide	C00455	nicotinate & nicotinamide metabolism	0.42276	-1.2421	0.010448	1.981
dCTP-nega	C00458	pyrimidine metabolism	0.46269	-1.1119	0.004728	2.3253
dGTP	C00286	purine metabolism	0.51939	-0.9451	0.099317	1.003
dGDP-nega	C00361	purine metabolism	0.53069	-0.91406	0.077495	1.1107
ADP-nega	C00008	purine metabolism	0.55566	-0.84773	0.094017	1.0268
NADPH-nega	C00005	glutathione metabolism	0.61037	-0.71225	0.099435	1.0025
IDP-nega	C00104	purine metabolism	0.63205	-0.66189	0.095918	1.0181
aminoimidazole carboxamide ribonucleotide	C04677	purine metabolism	0.64544	-0.63164	0.021033	1.6771
atrolactic acid	HMDB00475	phenylalanine metabolism	1.5241	0.60794	0.075853	1.12
thymine	C00178	pyrimidine metabolism	1.573	0.6535	0.018955	1.7223
D-glucosamine-6-phosphate	C00352	amino sugar & nucleotide sugar metabolism	1.6124	0.68925	0.11918	0.92381
nicotinamide riboside	C03150	nicotinate & nicotinamide metabolism	1.6263	0.70158	0.0008533	3.0689
cytosine	C00380	pyrimidine metabolism	1.9227	0.94312	0.0029985	2.5231
deoxyguanosine	C00330	purine metabolism	1.9346	0.95202	0.10065	0.99717
N-acetylputrescine	C02714	arginine & proline metabolism	2.0606	1.0431	0.052397	1.2807
cytidine	C00475	pyrimidine metabolism	2.2522	1.1714	0.0002413	3.6175
putrescine	C00134	arginine & proline metabolism	2.2827	1.1908	0.0058995	2.2292
D-sedoheptulose-1-7-phosphate	C05382	pentose phosphate pathway	2.4255	1.2783	0.087554	1.0577
dTMP	C00364	pyrimidine metabolism	3.5606	1.8321	0.0048334	2.3157
hypoxanthine	C00262	purine metabolism	5.5227	2.4654	0.044853	1.3482

Metabolites detectable in all DMSO control samples but not in all treated samples (shown are peak intensity values):

metabolites	DMSO_1	DMSO_2	DMSO_3	Torin2_1	Torin2_2	Torin2_3
FMN	13817.834	9204.5133	13128.728	NA	NA	5086.4902
cyclic bis(3->5) dimeric GMP	7676.6683	3390.8084	14429.984	4185.0821	NA	NA
succinyl-CoA-methylmalonyl-CoA-nega	5090.8746	5085.0194	8670.1861	NA	NA	NA
choline	2871318.1	804003.85	2266906.1	NA	NA	NA
histidinol	15249.437	5476.1406	10984.721	NA	NA	9324.3814
flavone	8964.2054	7859.0649	7875.8126	NA	NA	NA
5-methoxytryptophan	11870.832	7628.6091	13568.743	NA	NA	NA
diiodothyronine	8350.4798	6784.3105	4675.5421	16973.513	NA	NA
retinoic acid	14769.437	6658.804	3700.0403	NA	NA	8282.8993

Summary and interpretation: Compared to BT-549 cells treated with DMSO, cells treated with active drug for 6h exhibit decreased levels of both pyrimidine and purine deoxyribonucleotide triphosphates and/or their precursors including deoxycytidine triphosphate (dCTP), cytidine monophosphate (CMP), deoxythymidine diphosphate (dTDP), deoxyguanosine triphosphate (dGTP) and adenosine diphosphate (ADP), among others. The changes in metabolite levels are consistent with inhibition of both *de novo* synthesis and salvage pathways for pyrimidine and purine nucleotides.

- Increased levels of cytidine and cytosine suggest inhibition of pyrimidine salvage pathways.
- Decreased levels of carbamoyl phosphate, N-carbamoyl-L-aspartate and/or uridine triphosphate (UTP) suggest decreased *de novo* synthesis of pyrimidines.
- Increased levels of deoxythymidine monophosphate (dTMP) and decreased levels of deoxythymidine diphosphate (dTDP) are consistent with reduced activity of deoxythymidylate kinase, an enzyme that acts downstream of *de novo* synthesis and salvage pathways for pyrimidines.
- Increased levels of hypoxanthine, deoxyinosine and/or deoxyguanosine suggest inhibition of purine salvage pathways.
- Decreased levels of AICAR may reflect decreased *de novo* purine synthesis.